

Development of Area-Efficient Using Encoder Decoder and EDC For 5g LDPC Codes

Agastiya.A¹, Ms.A.Deepalakshmi M.E²

¹PG Scholar, M.E-VLSI Design, Surya Group of Institutions, Vikiravandi

²Assistant Professor/ECE, Surya Group of Institutions, Vikiravandi

Abstract-The fifth-generation (5G) new radio has used the low-density parity-check (LDPC) code as a highly promising error-correction code as the channel coding scheme. However, designing a high-performance decoder for 5G LDPC codes is extremely difficult since their intrinsic multiple degree-1 variable-nodes are prone to error. The problem is handled elegantly in this study by introducing a low-complexity check-node update algorithm, which considerably improves the dependability of check-to-variable messages. By implementing the proposed column degree modification approach, our decoder might outperform existing ones by 0.4dB. This research also provides an efficient 5G LDPC decoder design. Layer merging, split storage mechanism, and selective-shift structure are presented to benefit the special structure of 5G LDPC codes, allowing for a considerable decrease in decoding latency and area consumption. The results of implementation using 90-nm CMOS technology show that the suggested decoder architecture achieves an outstanding gain in throughput-to-area ratio, up to 173.3% when compared to traditional design.

Keywords: Low-density parity-check codes, 5G LDPC decoder, high-performance, VLSI implementation.

1. INTRODUCTION

Low-density parity-check codes have attracted considerable attention over the past several decades because of their remarkable error-correction performance and inherent parallelism for hardware implementation. LDPC codes also have been adopted in several industrial standards, including IEEE 802.11 [2], the second-generation satellite digital video broadcast (DVB-S2) [3], and advanced television system committee (ATSC) [4]. Recently, LDPC codes have been chosen as the 5G new radio (NR) channel, coding scheme in the enhanced mobile broadband (eMBB) scenario [5]. LDPC codes can perform close to the Shannon limit when paired with the belief propagation (BP) decoding algorithm [6]. However, the BP algorithm involves complex non-linear functions in check-node (CN)

processing, leading to large implementation complexity.

As an alternative, the min-sum (MS) algorithm [7] was proposed and became the primary solutions in practical applications. By approximating the non-linear functions with simple summation and comparison operations, the MS algorithm can get significant complexity reduction at the cost of obvious performance loss. By introducing the correction factor to decoding, the normalized MS (NMS) and offset MS (OMS) algorithms could offer a better balance between decoding complexity and performance [8].

This research paper targets the design of an area-efficient and high performance 5G LDPC decoder. In general, 5G LDPC codes are built from a concatenation of a high-rate LDPC code and a low-density generator matrix (LDGM) code [9]. Since the variable-nodes (VNs) in the LDGM part are degree-1 VNs which can only receive one check-to-variable (CTV) message in each iteration, they are very sensitive to the reliability of the received CTV messages, and so to the choice of the correction factor. Therefore, in fixed-point implementations with low quantization bits where the precision of correction factor is limited, the OMS decoder suffers from severe performance degradation [10].

Recently, the adapted MS (AMS) decoder [10] was proposed which targets fixed-point decoding. In 5G LDPC codes, the CNs connected to the degree-1 VNs are called extension checks and others are referred to core checks. Considering the fact that the degree-1 VNs are more likely to be erroneous when an imprecise offset factor is adopted, in the AMS decoder, the offset factor is only applied to core checks. Consequently, with low quantization bits, the AMS decoder could offer better performance than the MS and OMS decoders on 5G LDPC codes. To further improve the performance of 5G LDPC decoders, this article introduces an improved AMS (IAMS) algorithm. Starting from reducing the error-probability of degree-1 VNs, a modified CN-update

function is designed which considerably improves the reliability of CTV messages while maintaining the low-complexity property. Moreover, considering 5G LDPC codes are extremely irregular, a column degree adaptation strategy is proposed to manage the influence of the high-degree VNs on the decoding process. Simulation results on several 5G LDPC codes with different code rates and code lengths demonstrate that the proposed IAMS algorithm could offer an obvious performance improvement compared to existing ones, especially for codes with low to moderate code rates.

The implementation of LDPC decoders has been fully investigated [16]–[20]. In [17], the authors introduced a fully-parallel bit-parallel architecture with detailed optimizations for high-throughput applications. Since the complexity of the fully-parallel decoder is relatively high, the partially-parallel schedule, such as the layered schedule, has become the most popular one, which could use the up-to-date information from the current iteration, thereby doubling the speed of the decoding convergence. When the quasi-cyclic LDPC (QC-LDPC) codes are adopted, the CNs in the same block row of the base matrix are usually grouped into a single layer. In [18], an efficient reordered layered schedule was proposed to minimize the memory consumption. Moreover, to reduce the required number of iterations, the authors of [21] introduced a modified layered schedule for 5G LDPC codes, in which the processing order of layers is not sequential, but depends on the number of punctured edges and check-node degrees.

2. NOTATIONS AND PRELIMINARIES

A. Notations

An LDPC code is specified by a sparse $M \times N$ parity check matrix H , where M denotes the number of parity checks and N represents the number of code bits. The code rate $R = K/N = (N - M)/N$. LDPC codes can also be defined by bipartite Tanner graphs [22] which comprise a set of VNs and a set of CNs, corresponding to code bits and parity checks, respectively. Let $N(m)$ denote the set of VNs that participate in the m th check. Similarly, the neighbours set of the n th VN is denoted by $M(n)$. The number of neighbours connected with a VN is called column degree and with a CN is called row degree, denoted by d_v and d_c , respectively. An LDPC code is regular if the degrees of each set of nodes are the same, while degrees of an irregular

LDPC code vary according to some degree distributions. QC-LDPC codes have a structured H matrix that can be generated from an $M_b \times N_b$ base matrix HB . Each nonzero entry of HB can be expanded by circularly shifting a $Z \times Z$ identity matrix and each zero entry represents a $Z \times Z$ all-zero matrix, where Z denotes the expansion factor.

B. 5G LDPC Codes

To support a broad range of code lengths and rates, two rate-compatible base graphs, BG1 and BG2, are designed for 5G LDPC codes. These two base graphs have a similar structure while BG1 is targeted for larger information lengths ($500 \leq K \leq 8448$) and higher rates ($1/3 \leq R \leq 8/9$) and BG2 is targeted for smaller information lengths ($40 \leq K \leq 2560$) and lower rates ($1/5 \leq R \leq 2/3$). Fig. 1 shows the structure of base matrix BG2 which has 42 rows and 52 columns. The sub-matrix H_{core} is called the core part and the other three sub-matrices form the extension part. In both BG1 and BG2 matrices, H_{core} consists of the first four rows of the base matrix and adopts a dual diagonal structure for parity bits to simplify the encoding process. The extension part has an equal amount of VNs and CNs, and all extension VNs are degree-1 nodes. O denotes an all-zero matrix and I denote an identity matrix. The core checks usually have a higher row degree than the extension checks. The leftmost two columns of the base matrix correspond to the punctured bits, also known as the state bits. One important feature for 5G LDPC codes is that they are extremely irregular, which means there exists a significant difference in row degrees and column degrees. For instance, in base matrix BG2, d_v varies from 1 to 23 and d_c varies from 3 to 10.

C. Fixed-Point LDPC Decoding's

Assume an LDPC codeword $c = \{c_0, c_1, \dots, c_{N-1}\}$ is transmitted over the additive white Gaussian noise (AWGN) channel using the binary phase shift keying (BPSK) modulation, the received vector y is

$$y_i = x_i + n_i, \quad n_i \sim \mathcal{N}(0, \sigma^2), \quad i = 0, 1, \dots, N - 1, \quad (1)$$

where $x_i = 1 - 2c_i$ and n_i is a Gaussian random variable with zero mean and variance σ^2 . In fixed-point implementations, the quantized version of y , denoted by γ , is typically input to the decoders. Let Γ represent the input alphabet comprising of integers, and then we have $\gamma_i = [\mu \cdot y_i]_{\Gamma}$ where $\mu > 0$ is a constant referred to as the gain factor. $[x]_{\Gamma}$ returns the closest integer to x that belongs to Γ . Assume the input messages are expressed by q bits,

we have $\Gamma = \{-Q, \dots, -1, 0, 1, \dots, +Q\}$ where $Q = 2q-1 - 1$. Actually, $\mu = 2q$ means that all channel LLR values are shifted q bits to the left and then rounded to integers, which is the same as the usual quantization method when q fraction bits are preserved. Moreover, the introduced quantization method is more flexible because the values of μ could be optimized to other values besides $2q$ for better decoding performance [23].

The decoding process of the layered schedule is described as follows.

1) Initialization: Assign the values of the input vector γ to the APP vector $\tilde{\gamma}$. Moreover, all CTV messages $\alpha_{m,n}$ are initialized with zeros.

2) Iterative Process: In the layered schedule, each iteration comprises several decoding layers. The decoding is executed layer by layer and each layer has three steps.

Step 1 (VN update): In the t th iteration, the variable-to check (VTC) message $\beta^{(t)}_{n,m}$ is calculated by

$$\beta_{n,m}^{(t)} = \lfloor \tilde{\beta}_{n,m}^{(t)} \rfloor_{\Gamma} = \lfloor \tilde{\gamma}_n^{(t)} - \alpha_{m,n}^{(t-1)} \rfloor_{\Gamma}.$$

Step 2 (CN update): In the BP decoding, the CTV message is given by

$$\alpha_{m,n}^{(t)} = \tau_{m,n}^{(t)} \cdot \phi \left(\sum_{n' \in \mathcal{N}(m) \setminus n} \phi(|\beta_{n',m}^{(t)}|) \right),$$

Considering $\phi^{-1}(x) = \phi(x)$ and the magnitude of $\alpha^{(t)}_{m,n}$ is dominated by the minimum input $|\beta^{(t)}_{n',m}|$ [24], the MS simplifies (3) according to

$$\begin{aligned} \alpha_{m,n}^{(t)} &\simeq \tau_{m,n}^{(t)} \cdot \phi \left(\phi \left(\min_{n' \in \mathcal{N}(m) \setminus n} |\beta_{n',m}^{(t)}| \right) \right) \\ &= \tau_{m,n}^{(t)} \cdot \min_{n' \in \mathcal{N}(m) \setminus n} |\beta_{n',m}^{(t)}|. \end{aligned}$$

$$\alpha_{m,n}^{(t)} = \tau_{m,n}^{(t)} \cdot \max \left(\min_{n' \in \mathcal{N}(m) \setminus n} |\beta_{n',m}^{(t)}| - \lambda, 0 \right),$$

Step 3 (APP update): In order to achieve better precision, $\tilde{\beta}^{(t)}_{n,m}$ in (2) is used to update APP values according to

$$\tilde{\gamma}_n^{(t)} = \lfloor \alpha_{m,n}^{(t)} + \tilde{\beta}_{n,m}^{(t)} \rfloor_A,$$

$$\hat{c}_n^{(t)} = HD(\tilde{\gamma}_n^{(t)}) = \begin{cases} 0, & \tilde{\gamma}_n^{(t)} \geq 0 \\ 1, & \tilde{\gamma}_n^{(t)} < 0. \end{cases}$$

3) THE PROPOSED IAMS DECODING ALGORITHM

A. The Modified CN-Update Function

As mentioned above, all extension VNs in 5G LDPC codes are with degree-1 and each is connected to a

unique CN. Consequently, these VNs only receive one CTV message in each iteration so they are sensitive to the reliability of CTV messages and the choice of offset factor. In fixed-point implementations, the offset factor is generally not optimal so the reliability of CTV messages is limited due to the limited bit representation of messages, which is the main reason for the severe performance degradation appearing in fixed-point OMS decoder. In order to improve the performance of 5G LDPC decoders, we propose a new CN-update function in this subsection to improve the reliability of CTV messages, and thus efficiently benefits the performance improvement of 5G LDPC decoders. Denote the first and second minimum magnitudes of the input VTC messages in a CN by \min_1 and \min_2 , respectively.

In order to maintain the low computation complexity, we only use these two values which are available in conventional MS decoder to design a new CN-update function. Let idx_1 and idx_2 be the indices of VNs corresponding to \min_1 and \min_2 , respectively. $I(m)$ is defined as $I(m) = \{\text{idx}_1, \text{idx}_2\}$ and $\bar{I}(m) = \mathcal{N}(m) \setminus I(m)$. Observing (3) we notice that, for $n \in \bar{I}(m)$, both \min_1 and \min_2 are extrinsic VTC messages that are used to calculate the CTV message $\alpha^{(t)}_{m,n}$. Since the magnitude of $\alpha^{(t)}_{m,n}$ is dominated by the minimum magnitude of extrinsic VTC messages, a sufficient precision can be achieved if the first and second minimum magnitudes of the extrinsic VTC messages are both employed to approximate the CN-update function of the BP algorithm. Therefore, for $n \in \bar{I}(m)$, we approximate the CN-update function shown in (3) to

$$\alpha_{m,n}^{(t)} = \tau_{m,n}^{(t)} \cdot \phi \left(\phi(\min_1) + \phi(\min_2) \right).$$

$$\alpha_{m,n}^{(t)} = \tau_{m,n}^{(t)} \cdot (\min_1 \boxplus \min_2),$$

$$\lambda = \log \frac{1 + e^{-\Delta}}{1 + e^{-(2a+\Delta)}}.$$

Since \min_1 and \min_2 are both non-negative integers in fixed-point implementations, a and a are also non-negative integers. Therefore, we can conclude that $\lambda \geq 0$ so the quantized version of λ is

$$\lambda = \lfloor \log \frac{1 + e^{-\Delta}}{1 + e^{-(2a+\Delta)}} + \frac{1}{2} \rfloor.$$

Based on this property, the offset factor for $n \in \bar{I}(m)$ can be determined according to \min_1 and \min_2 . For $n \in I(m)$, we cannot obtain a more precise correction factor only based on \min_1 and \min_2 . Since MS decoder performs better than OMS decoder on 5G

LDPC codes in fixed-point implementations [10], λ is set to 0 for $n \in I(m)$. The proposed CN-update function is shown in (10), which still remains the low-complexity property

$$a_{m,n}^{(t)} = \begin{cases} \tau_{m,n}^{(t)} \cdot \min_2, & n = idx_1 \\ \tau_{m,n}^{(t)} \cdot \min_1, & n = idx_2 \\ \tau_{m,n}^{(t)} \cdot \max(\min_1 - 1, 0), & n \in \tilde{I}(m) \ \& \ \Delta = 0 \\ \tau_{m,n}^{(t)} \cdot \min_1, & n \in \tilde{I}(m) \ \& \ \Delta \neq 0. \end{cases}$$

To demonstrate the effectiveness of the proposed CN-update function, the mismatch probabilities of different CN-update functions are shown in Fig. 2, where the exchanged messages are quantized to 4 bits, i.e., $q = 4$. Therefore, the values of $|\beta_{n,m}|$ can only be $0 \sim 7$ so the total number of combinations of the received messages in a degree- dc CN is $8dc$ ($2^{(q-1)} \cdot dc$). For each case, if the CTV value calculated by the tested decoder is not equal to the CTV value calculated by the 4-bit quantized BP decoder, we consider this case as a mismatch case. The mismatch probability is obtained by testing all $8dc$ cases and then calculating the proportion of mismatch cases.

B. Column Degree Adaptation

As stated before, 5G LDPC codes are extremely irregular and there exists a wide variation in column degrees. In base matrix BG2, the column degree varies from 1 to 23 and from 1 to 30 in BG1. With more neighbor CNs, the high degree VNs usually have larger APP magnitudes, which are called strong messages. These strong messages can be helpful or harmful to the decoding process, depending on whether they are correct or not. In the waterfall region where many bits are received incorrectly, the incorrect strong messages tend to negatively influence the correction of the received bits. In the error-floor region where the channel conditions are good and trapping-sets dominate the decoding performance [25], the correct strong messages can overcome the incorrect messages in trapping-sets and thus contribute to improving the decoding performance [26]. Therefore, the requirement of strong messages is different in different SNR regions.

In order to manage the influence of strong messages on the decoding process, we propose a column degree adaptation strategy in which the CTV messages passed to different VNs from a CN are computed non-uniformly. Observing (5) and (10) we can conclude that the magnitudes of CTV messages computed by the OMS decoding are generally

smaller than those by the proposed CN-update function. To limit the magnitudes' growth of strong messages, the CTV messages transmitted to the VNs whose degrees are larger than threshold D is computed using the CN-update function of the OMS decoding rather than the proposed CN-update function.

To avoid over-correction to strong messages, the column degree adaptation is only applied to core checks, whose CTV messages show a lower mismatch probability than those of extension checks when applying the OMS decoding, as shown in Fig. 2. Consequently, the influence of strong messages to the decoding process could be managed to some extent by adjusting parameter D and the decoding performance could get a better balance in the waterfall and error-floor regions. Moreover, one can select a proper D to get the best performance in the required SNR region.

Considering the degrees of bits in the first two groups are much larger than others, these bits have more chances to be corrected so the first two groups show the best performance, especially for the OMS and M2 decoders. Since Fig. 3 shows the simulation results in the low SNR region where many bits are received incorrectly, the propagation of incorrect strong messages has larger negative influence to decoding than the imprecise offset factor. Therefore, the OMS decoder performs better than the MS decoder. However, they both perform worse than the AMS decoder [10], which is the state-of-the-art one for 5G LDPC codes in fixed-point. Moreover, it can be seen that for all groups, the M1 and M2 decoders exhibit better performance than the AMS decoder. With the help of the proposed column degree adaptation, M2 significantly improves the decoding performance of the M1 decoder, proving the effectiveness of the proposed column degree adaptation.

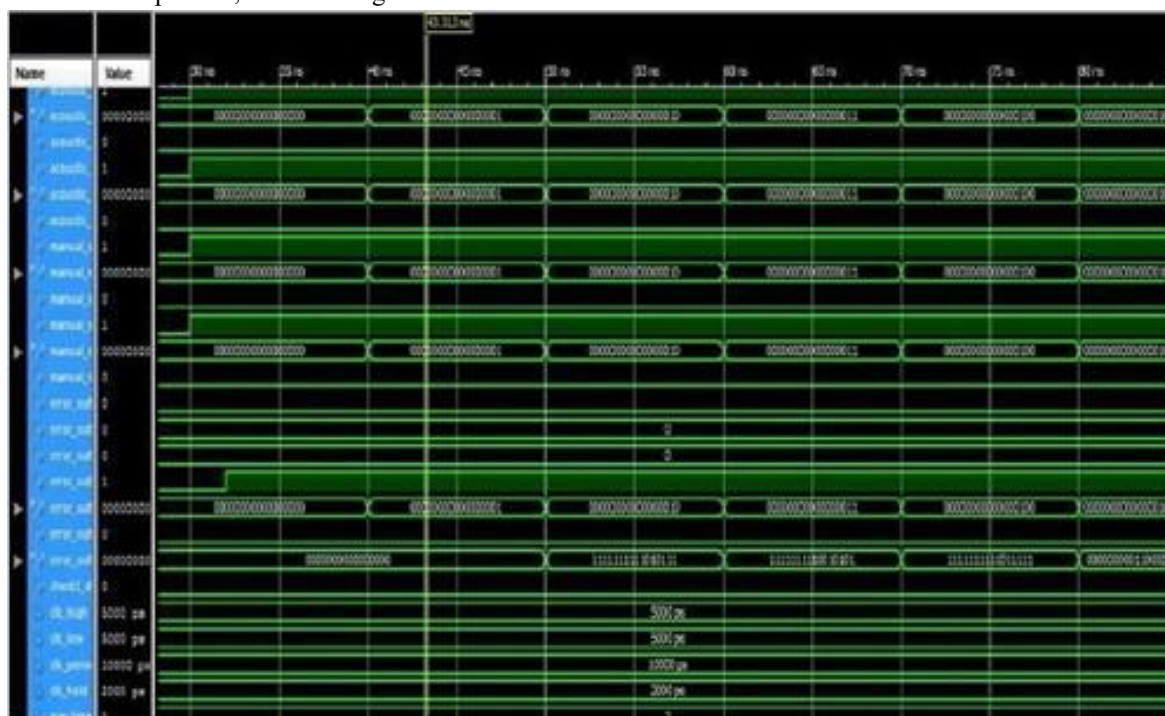
4) RESULTS AND DISCUSSIONS

The decoding performance of the proposed IAMS algorithm is illustrated and compared to the MS, OMS, and AMS decodings. All decodings take the layered schedule. In practical applications, the number of quantization bits used in LDPC decoders is usually no more than 6 in order to reduce the area and power consumption. Therefore, the quantization parameters are set to $(q, \tilde{q}) = (4, 6)$ in this work. Moreover, the performance of the floating-point MS and OMS algorithms are shown for reference, which also

take the layered schedule. The offset value for the floating-point OMS decodings is set to 0.2. The simulation results are obtained through Monte-Carlo simulations that generate at least 100 error frames for each plotted point. Since the maximum number of iterations is typically less than 20 in practical implementations considering the throughput requirement while the decoders need about 100 iterations to be saturated, Fig. 7.1 show the simulation results on the BG code to correct the before error.

each decoding are fixed and optimized by simulations to find the value which performs best when $FER = 10^{-7}$, where the test step is set to 0.05. The optimal values for the OMS, MS, AMS, and IAMS decoders are 1.3, 1.1, 0.85, and 0.8, respectively. Due to the imprecise offset factor, the OMS decoder suffers from server performance degradation under quantization, which could be compensated by increasing one bit of quantization length. Compared to the AMS decoding, the proposed IAMS decoding shows a much better performance.

For a fair comparison, the channel gain factors for



Development of Area-Efficient Using Encoder Decoder and ECC for 5G LDPC Codes

we explore the effect of limiting the maximum number of iterations on different decodings, where I_{tmax} increases from 0 to 1. The code is adopted and two points, 2.0dB and 2.6dB, are considered. The performance in the waterfall region where the random-like errors are main causes of decoding failures. As shown in by increasing the maximum number of iterations, most of these errors can be corrected and the

decoding performance is improved. Since a smaller D has better capability to limit the magnitudes growth of strong random-like errors, when I_{tmax} is not sufficient, the IAMS decoding paired with has a better performance. Also, because the overestimation of CTV messages encourages the magnitude growth of errors, the MS decoding shows poor performance and converges slowly at this point.



Error Correction and Error Detection

When sufficiently large, the decoding performance is dominated by trapping-sets, which are main reasons for the error-floor phenomenon. Fig. 7.2 shows the performance under different iteration limits in the error-floor region. Moreover, the IAMS decoding paired with can surpass that with in performance within a smaller number of iterations. The value evolution when the IAMS algorithm with is applied. The bits belonging to the collected trapping-set are marked with red squares and others with black circles. Assume the all-zero code word is transmitted using the BPSK modulation. Accordingly, nonnegative APP values are interpreted as correct and negative values denote faults. As can be seen, the decoder cannot escape from the trapping- set once it is captured. By increasing the value of D, more core checks could be processed by the proposed CN-update function rather than the OMS decoding. This explains why the IAMS decoding could perform better when paired with in the error-floor region. However, in order to balance the decoding performance in the waterfall region, is not the larger the better. Also, the correction of random-like errors in early iterations will be damaged by an excessive. Compared to the case when, the second connected CN sends a slightly larger correct CTV message to this VN when and thus, the corresponding bit could be correctly recovered. Consequently, this code word can be successfully decoded when. This explains why the IAMS decoding could perform better when paired with in the error-floor region. However, in order to balance the decoding

performance in the waterfall region, D is not the larger the better. Also, the correction of random-like errors in early iterations will be damaged by an excessive D. The encoded data from the memory and decodes the corresponding encoded data using majority logic decoding. The comparator is used to compare the input data and the decoded data. Thus the decoder is designed and verified using Modelsim simulator.

5) CONCLUSION

In this paper, we offer the enhanced adapted minimum method, a high-performance decoding technique for fixed-point decoding of 5G LDPC codes. A novel CN-update function is devised to lower the error-probability of degree-1 VNs, and the column degree adaption is presented to relieve the excessive rise of posterior probability in high-degree VNs. As a consequence, the suggested decoder may surpass the state-of-the-art AMS decoder in FER performance by 0.4dB. We also provide a high-performance design for 5G LDPC decoders. The layer merging approach is first used, which is based on the orthogonality property of the basis matrix. The divided storage strategy is then used to further minimise the cost of CTV memory. Finally, the selective-shift structure and message reordering approach are used to optimise the connectivity blocks. The results of implementation show that the suggested design may enhance the throughput-to-area ratio by 173.3%.

REFERENCES

- [1] R. G. Gallager, "Low-density parity-check codes," *IRE Trans. Inf. Theory*, vol. 8, no. 1, pp. 21–28, Jan. 1962.
- [2] IEEE 802.11n Wireless LAN Medium Access Control MAC and Physical Layer PHY Specifications, Standard IEEE 802.11n-D2.0, 2007.
- [3] Second Generation Framing Structure, Channel Coding and Modulation Systems for Broadcasting, Interactive Services, News Gathering and Other Broadband Satellite Applications (DVB-S2), ETSI, Sophia Antipolis, France, 2009.
- [4] Standard: Synchronization Standard for Distributed Transmission, ATSC, Boston, MA, USA, 2007. [5] Multiplexing and Channel Coding, document TS 38.212 V15.0.0, 3GPP, Dec. 2017.
- [6] T. J. Richardson and R. L. Urbanke, "The capacity of low-density parity-check codes under message-passing decoding," *IEEE Trans. Inf. Theory*, vol. 47, no. 2, pp. 599–618, Feb. 2001.
- [7] M. P. C. Fossorier, M. Mihaljevic, and H. Imai, "Reduced complexity iterative decoding of low-density parity check codes based on belief propagation," *IEEE Trans. Commun.*, vol. 47, no. 5, pp. 673–680, May 1999.
- [8] J. Chen, A. Dholakia, E. Eleftheriou, M. P. C. Fossorier, and X.-Y. Hu, "Reduced-complexity decoding of LDPC codes," *IEEE Trans. Commun.*, vol. 53, no. 8, pp. 1288–1299, Aug. 2005.
- [9] T. Richardson and S. Kudekar, "Design of low-density parity check codes for 5G new radio," *IEEE Commun. Mag.*, vol. 56, no. 3, pp. 28–34, Mar. 2018.
- [10] K. Le Trung, F. Ghaffari, and D. Declercq, "An adaptation of min-sum decoder for 5G low-density parity-check codes," in *Proc. IEEE Int. Symp. Circuits Syst. (ISCAS)*, Sapporo, Japan, May 2019, pp. 1–5. [11] LDPC Decoding With Adjusted Min-Sum, document R1-1610140, TSG RAN WG1 #86bis, 3GPP, Qualcomm Incorporated, Lisbon, Portugal, Oct. 2016.
- [12] W. Zhou and M. Lentmaier, "Generalized two-magnitude check node updating with self correction for 5G LDPC codes decoding," in *Proc. 12th Int. ITG Conf. Syst., Commun. Coding*, Rostock, Germany, Mar. 2019, pp. 1–6.
- [13] K. Sun and M. Jiang, "A hybrid decoding algorithm for low-rate LDPC codes in 5G," in *Proc. 10th Int. Conf. Wireless Commun. Signal Process. (WCSP)*, Hangzhou, China, Oct. 2018, pp. 1–5.
- [14] X. Wu, M. Jiang, and C. Zhao, "Decoding optimization for 5G LDPC codes by machine learning," *IEEE Access*, vol. 6, pp. 50179–50186, 2018.
- [15] C. Jones, E. Valles, M. Smith, and J. Villasenor, "Approximate \square MIN* constraint node updating for LDPC code decoding," in *Proc. IEEE Mil. Commun. Conf. (MILCOM)*, Boston, MA, USA, Oct. 2003, pp. 157–162.
- [16] K. Zhang, X. Huang, and Z. Wang, "A high-throughput LDPC decoder architecture with rate compatibility," *IEEE Trans. Circuits Syst. I, Reg. Papers*, vol. 58, no. 4, pp. 839–847, Apr. 2011.
- [17] C.-C. Cheng, J.-D. Yang, H.-C. Lee, C.-H. Yang, and Y.-L. Ueng, "A fully parallel LDPC decoder architecture using probabilistic min-sum algorithm for high-throughput applications," *IEEE Trans. Circuits Syst. I, Reg. Papers*, vol. 61, no. 9, pp. 2738–2746, Sep. 2014.
- [18] H.-C. Lee, M.-R. Li, J.-K. Hu, P.-C. Chou, and Y.-L. Ueng, "Optimization techniques for the efficient implementation of high-rate layered QC-LDPC decoders," *IEEE Trans. Circuits Syst. I, Reg. Papers*, vol. 64, no. 2, pp. 457–470, Feb. 2017.
- [19] I. Tsatsaragkos and V. Paliouras, "A reconfigurable LDPC decoder optimized for 802.11n/AC applications," *IEEE Trans. Very Large Scale Integr. (VLSI) Syst.*, vol. 26, no. 1, pp. 182–195, Jan. 2018.
- [20] T. T. Nguyen-Ly, V. Savin, K. Le, D. Declercq, F. Ghaffari, and O. Boncalo, "Analysis and design of cost-effective, high-throughput LDPC decoders," *IEEE Trans. Very Large Scale Integr. (VLSI) Syst.*, vol. 26, no. 3, pp. 508–521, Mar. 2018.